Inorganic Chemistry

Article

pubs.acs.org/IC

Stabilizing Radical Cation and Dication of a Tetrathiafulvalene Derivative by a Weakly Coordinating Anion

Feng Gao,[†] Fei-Fei Zhu,[†] Xing-Yong Wang,[†] Yan Xu,[‡] Xin-Ping Wang,*[,†] and Jing-Lin Zuo*[,†]

[†]State Key Laboratory of Coordination Chemistry, School of Chemistry and Chemical Engineering, Nanjing National Laboratory of Microstructures, Nanjing University, Nanjing 210093, P. R. China

[‡]College of Chemistry and Chemical Engineering, Nanjing University of Technology, Nanjing, 210009, P. R. China

Supporting Information

ABSTRACT: After the chemical oxidation of the neutral tetrakis(methylthio)tetrathiafulvalene (TMT-TTF, **1**) by specific oxidation agents with weakly coordinating anion, $[Al(OR_F)_4]^-$ [OR_F = $OC(CF_3)_3$], the radical cation TMT-TTF$^{\bullet+}$ ($\mathbf{1}^{\bullet+}$) and dication TMT-TTF^{2+} ($\mathbf{1}^{2+}$) were successfully stabilized and isolated. All the compounds are well-soluble in some solvents and have been systematically investigated by absorption spectra, ^{1}H NMR, electron paramagnetic resonance (EPR) measurements. Their crystal structures and electronic properties have been studied in conjunction with theoretical calculation. The synthetic approach for chemical oxidation by specific salts of weakly coordinating anions is useful for stable radical cations of tetrathiafulvalene (TTF) and its derivatives in both solution and solid state, which will extend the further research, including structure−property relations on stable radicals for TTF derivatives and new functional materials based on them.

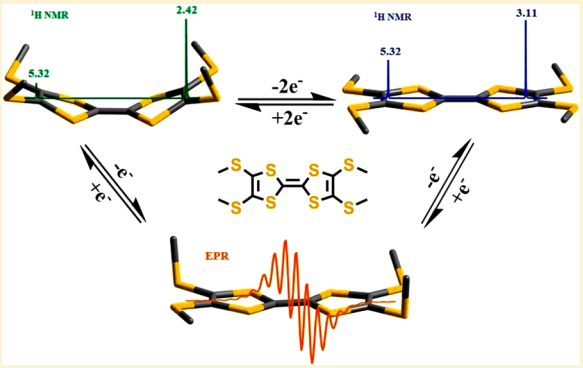

INTRODUCTION

Molecule-based materials with tunable conductive, magnetic, or optical properties have attracted much attention from both the fundamental scientific view and technological applications.[1] As a representative, tetrathiafulvalene (TTF) and its derivatives, well-known sulfur-rich organic molecules, have been extensively studied as organic conductors and molecular optoelectronic materials owing to their unique π-donor properties.[2,3] By reacting with various organic or inorganic acceptors, these electroactive molecules are inclined to form charge transfer compounds, in which some species that possess unpaired electrons, i.e., radicals, can be found. Such radical cation salts would provide unique models to probe the structural and electronic consequences of mixing π electrons and spins. More importantly, the assembly of TTF-based radicals with metal ions, especially paramagnetic metal ions, will construct new functional materials with intriguing structures and interesting properties.[4]

Recently, the isolation of stable organic radicals is an area of high current interest, and their structure and electronic properties have been extensively studied in conjunction with theoretical calculation.[4a,5] For TTF-based organic radical compounds, they are usually prepared by one-electron or partially electrochemical or chemical oxidation on the neutral molecule.[4a,h,6,7] However, two-electron oxidation of TTF derivatives and their stable dications in the solid state are rarely studied.[8] To the best of our knowledge, it is difficult to investigate the physical or chemical properties for the radical or dicationic TTF species due to their stability and solubility in solution state. That is, it is still the key challenge to stabilize the soluble radical or dicationic species for TTF derivatives. Additionally, it is also important to fully explore novel and stable structural motifs with successively forming both a radical cation and a dication.

In our previous work, the weakly coordinating anion $[Al(OR_F)_4]^-$ [OR_F = $OC(CF_3)_3$] (Scheme 1, right) has been demonstrated as an efficient tool to stabilize reactive organic

Scheme 1. Molecular Structures of Tetrakis(methylthio)tetrathiafulvalene (TMT-TTF, 1) and Polyfluoroalkoxyaluminate Anion $[Al(OR_F)_4]^-$ [OR_F = $OC(CF_3)_3$]

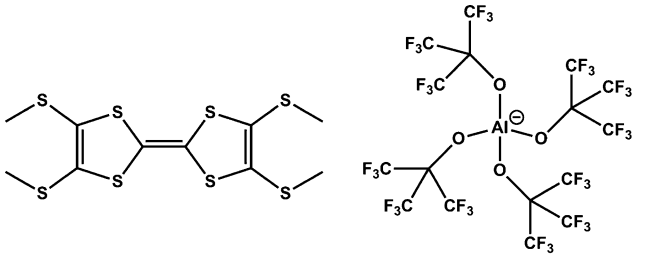

TMT-TTF (1)

$[Al(OR_F)_4]^-$ (OR_F = $OC(CF_3)_3$)

Received: March 16, 2014
Published: May 2, 2014

   dx.doi.org/10.1021/ic5006117 | Inorg. Chem. 2014, 53, 5321−5327

Table 1. Crystallographic Data for All of the Compounds

	1	$1^{\bullet+}$	1^{2+}
formula	$C_{10}H_{12}S_8$	$C_{104}H_{48}Al_4F_{144}O_{16}S_{32}$	$C_{21}H_6AlF_{36}O_4S_4$
fw	388.68	5423.26	1161.48
cryst syst	monoclinic	triclinic	orthorhombic
space group	$P2_1/n$	$P\bar{1}$	*Pbca*
a, Å	13.876(3)	12.7865(18)	19.443(2)
b, Å	7.7082(18)	18.846(3)	17.8404(19)
c, Å	15.541(4)	19.209(3)	21.047(2)
α, deg	90	88.4690(17)	90
β, deg	106.999(2)	78.0730(16)	90
γ, deg	90	87.4090(16)	90
V, Å^3	1589.6(6)	4523.7(11)	7300.6(13)
Z	4	1	8
ρ_{calcd}, g cm^{-3}	1.624	1.991	2.113
T/K	123(2)	123(2)	123(2)
μ, mm^{-1}	1.102	0.599	0.503
θ, deg	2.34−25.50	1.76−25.00	2.09−26.00
F(000)	800	2660	4520
index ranges	$-16 \le h \le 16$	$-15 \le h \le 13$	$-23 \le h \le 23$
	$-9 \le k \le 7$	$-22 \le k \le 22$	$-22 \le k \le 22$
	$-18 \le l \le 18$	$-13 \le l \le 22$	$-25 \le l \le 16$
data/restraints/params	2937/0/163	15527/1257/1285	7155/6/624
GOF (F^2)	1.052	1.362	1.026
R_1,[a] wR_2[b] [$I > 2\sigma(I)$]	0.0262, 0.0909	0.1003, 0.2924	0.0352, 0.0880
R_1,[a] wR_2[b] (all data)	0.0314, 0.1159	0.1296, 0.3286	0.0420, 0.0941

[a] $R_1 = \sum||F_0| - |F_c||/\sum|F_0|$. [b] $wR_2 = [\sum w(F_0^2 - F_c^2)^2/\sum w(F_0^2)^2]^{1/2}$.

Table 2. Selected Bond Lengths (Å) and Bond Angles (deg) for $1^{\bullet+}$

bond distances (Å)			
C(33)−C(36)	1.393(12)	C(43)−C(46)	1.400(12)
C(34)−C(35)	1.375(12)	C(47)−C(48)	1.333(13)
C(37)−C(38)	1.345(13)	C(44)−C(45)	1.349(11)
S(1)−C(33)	1.714(9)	S(9)−C(43)	1.727(9)
S(1)−C(35)	1.747(8)	S(9)−C(45)	1.733(8)
S(2)−C(33)	1.715(9)	S(10)−C(43)	1.702(9)
S(2)−C(34)	1.754(8)	S(10)−C(44)	1.735(8)
S(3)−C(39)	1.805(11)	S(11)−C(49)	1.837(11)
S(4)−C(40)	1.826(13)	S(12)−C(50)	1.835(9)
S(5)−C(36)	1.747(8)	S(13)−C(46)	1.706(8)
S(5)−C(38)	1.762(8)	S(13)−C(48)	1.750(9)
S(6)−C(36)	1.695(8)	S(14)−C(46)	1.735(8)
S(6)−C(37)	1.733(8)	S(14)−C(47)	1.750(9)
S(7)−C(41)	1.806(12)	S(15)−C(51)	1.800(11)
S(8)−C(42)	1.811(11)	S(16)−C(52)	1.797(11)
bond angles (deg)			
S(1)−C(33)−C(36)	121.4(7)	S(13)−C(46)−C(43)	121.9(6)
S(1)−C(33)−S(2)	116.2(5)	S(13)−C(46)−S(14)	116.1(5)
C(33)−S(2)−C(34)	96.2(4)	C(46)−S(14)−C(47)	94.4(4)
C(33)−S(1)−C(35)	95.3(4)	C(46)−S(13)−C(48)	95.3(4)
C(34)−S(3)−C(39)	101.4(5)	C(48)−S(16)−C(52)	102.1(5)
C(35)−S(4)−C(40)	100.2(5)	C(47)−S(15)−C(51)	103.2(5)
S(5)−C(36)−C(33)	120.1(7)	S(9)−C(43)−C(46)	123.0(7)
S(5)−C(36)−S(6)	115.6(4)	S(9)−C(43)−S(10)	115.6(5)
C(36)−S(5)−C(38)	95.1(4)	C(43)−S(9)−C(45)	95.4(4)
C(36)−S(6)−C(37)	96.0(4)	C(43)−S(10)−C(44)	95.7(4)
C(38)−S(8)−C(42)	103.4(5)	C(44)−S(11)−C(49)	98.8(4)
C(37)−S(7)−C(41)	100.8(5)	C(45)−S(12)−C(50)	101.8(4)

radical cations and dications.[9] In this paper, we choose one of the typical TTF derivatives, tetrakis(methylthio)-tetrathiafulvalene (TMT-TTF, **1**, Scheme 1, left), to successfully isolate the corresponding radical cation TMT-TTF$^{\bullet+}$ ($\mathbf{1}^{\bullet+}$)

dx.doi.org/10.1021/ic5006117 | Inorg. Chem. 2014, 53, 5321−5327

Table 3. Selected Bond Lengths (Å) and Bond Angles (deg) for 1^{2+}[a]

bond distances (Å)			
C(5)−C(5)#1	1.427(4)	C(3)−S(2)	1.711(2)
C(2)−C(3)	1.394(3)	C(2)−S(3)	1.722(2)
C(5)−S(1)	1.701(2)	C(3)−S(4)	1.717(2)
C(5)−S(2)	1.703(2)	C(1)−S(3)	1.797(3)
C(2)−S(1)	1.710(2)	C(4)−S(4)	1.796(2)
bond angles (deg)			
S(1)−C(5)−C(5)#1	122.8(2)	C(1)−S(3)−C(2)	102.22(12)
S(2)−C(5)−C(5)#1	122.5(2)	C(3)−S(4)−C(4)	102.39(11)
S(1)−C(5)−S(2)	114.63(12)		

[a]Symmetry transformations used to generate equivalent atoms: #1 $-x, -y + 2, -z$.

and dication TMT-TTF^{2+} ($\mathbf{1}^{2+}$) by a conventional chemical oxidation method. All the compounds have been systematically investigated by UV−vis−NIR, ^{1}H NMR, electron paramagnetic resonance (EPR), and single crystal X-ray diffraction measurements. Our results extend the further research on structure−property relations for stable organic radicals of TTF derivatives.

EXPERIMENTAL SECTION

General Information. All experiments were carried out under a nitrogen atmosphere by using standard Schlenk techniques and a glovebox. Solvents were dried prior to use. $AgSbF_6$ and $NOSbF_6$ were purchased from Alfa Aesar and used upon arrival. Starting materials, TMT-TTF (**1**), $Li[Al(OR_F)_4]$, and $Ag[Al(OR_F)_4]$ were synthesized according to the published methods.[10,11] The ^{1}H NMR spectra were recorded using a Bruker DRX-500 in ppm downfield from Me_4Si. EPR spectra were obtained using a Bruker EMX10/12 variable-temperature apparatus. UV−vis−NIR spectra were obtained with a UV-3600 spectrophotometer. Cyclic voltammetry was performed with an Im6eX electrochemical analytical instrument by using platinum as the working and counter electrodes, a Ag/AgCl electrode containing saturated KCl solution as the reference electrode, and 0.1 M n-Bu_4NClO_4 as the supporting electrolyte. Elemental analysis was carried out with an Elementar Vario MICRO analyzer. Melting points were determined with an X-4 digital micro melting point apparatus.

X-ray Crystallography. All the crystal structures were determined at 123 K on a Bruker APEX DUO CCD diffractometer using monochromated Mo Kα radiation (λ = 0.710 73 Å). Integrations were performed with SAINT.[12] Absorption corrections were applied using the SADABS program.[13] The crystal structures were solved by direct methods and refined by full-matrix least-squares based on F^2 using the SHELXTL program.[14] All hydrogen atom positions were calculated geometrically and were riding on their respective atoms. Anisotropic refinement was not performed for the disordered atoms. More details for the data collections and structure refinements are given in Table 1. The selected bond lengths and bond angles are listed in Tables 2, 3, and S1 (Supporting Information) [CCDC reference numbers 991286 ($\mathbf{1}^{\bullet+}$) and 991285 ($\mathbf{1}^{2+}$)].

Computational Details. All the geometry optimizations were carried out at the (U)B3LYP/6-31G(d) level of theory. The UV−vis−NIR absorption spectra were calculated using the TD-DFT method at the (U)B3LYP/6-31G(d) level of theory. All calculations were performed with the Gaussian 09 program suite.[15]

Synthesis of $\mathbf{1}^{\bullet+}$. The reaction mixture of **1** (0.106 g, 0.27 mmol) and $Ag[Al(OR_F)_4]$ (0.292 g, 0.27 mmol) in 35 mL of CH_2Cl_2 was stirred at room temperature overnight. The resultant brown solution was filtered to remove the gray precipitate (Ag metal). The filtrate was then concentrated and stored at around −10 °C for several days to afford brown crystals. Yield: 0.215 g, 58.5%. Mp: 151−152 °C. Anal. Calcd for $C_{26}H_{12}AlF_{36}O_4S_8$ (%): C, 23.03; H, 0.89. Found: C, 22.85; H, 1.15. Selected UV−vis (CH_2Cl_2, λ_{max}/nm): 873, 484, 458, 333, and 257.

Synthesis of $\mathbf{1}^{2+}$. The reaction mixture of **1** (0.106 g, 0.27 mmol), $NOSbF_6$ (0.144 g, 0.54 mmol), and $Li[Al(OR_F)_4]$ (0.529 g, 0.54 mmol) in 60 mL of CH_2Cl_2 was stirred at room temperature overnight. The resultant blue-purple solution was filtered to remove the white precipitate ($LiSbF_6$). The filtrate was then concentrated and stored at around −20 °C for several days to afford blue-green crystals. Yield: 0.2305 g, 73.1%. Mp: 245−246 °C. Anal. Calcd for $C_{42}H_{12}Al_2F_{72}O_8S_8$ (%): C, 21.72; H, 0.52. Found: C, 21.43; H, 0.81. Selected UV−vis (CH_2Cl_2, λ_{max}/nm): 857, 489, 458, and 254. ^{1}H NMR (500 MHz, $C_2D_2Cl_2$, 293 K): δ (ppm) 3.11 (s, 12H, SCH_3).

RESULTS AND DISCUSSION

Synthesis and Characterization. TMT-TTF (**1**) was synthesized according to a classically organic homocoupling reaction. The electrochemical property has been investigated by cyclic voltammetry (Figure S1, Supporting Information). It exhibits two-step reversible single-electron oxidations corresponding successively to the formation of a radical cation ($\mathbf{1}^{\bullet+}$) and a dication fragment ($\mathbf{1}^{2+}$), confirming its redox activities. By using a weakly coordinating anion $[Al(OR_F)_4]^-$, we succeeded in stabilizing reactive tetrathiafulvalene-based radical cation and dication. The reaction of equimolar TMT-TTF and $Ag[Al(OR_F)_4]$ in CH_2Cl_2 resulted in the formation of TMT-TTF$^{\bullet+}$, but no corresponding dication fragment (TMT-TTF^{2+}) can be obtained upon further oxidation with 2 equiv of $Ag[Al(OR_F)_4]$, suggesting the weak oxidant ability of Ag(I) in this process. So the stronger oxidant composition ($NOSbF_6$ and $Li[Al(OR_F)_4]$) was used and we successfully achieved the conversion from neutral TMT-TTF to a dication TMT-TTF^{2+} in higher yield.

Table 4. Summary of Important Structural Parameters for All of the Compounds

structural parameter	**1**	$\mathbf{1}^{\bullet+}$	$\mathbf{1}^{2+}$
central C=C bond distance (Å)	1.338(3)	1.393(12), 1.400(12)	1.427(4)
av S−C_{CH_3} bond distance (Å)	1.808	1.815	1.796
dihedral angle for TTF core (deg)	49.63(7)	6.13(11), 7.20(13)	0

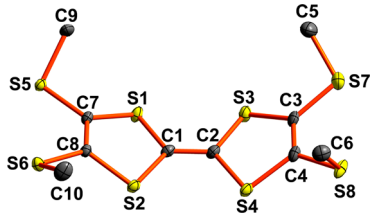

Figure 1. ORTEP diagram of **1** drawn at the 50% probability level. H atoms are omitted for clarity (S, yellow; C, gray).

dx.doi.org/10.1021/ic5006117 | Inorg. Chem. 2014, 53, 5321−5327

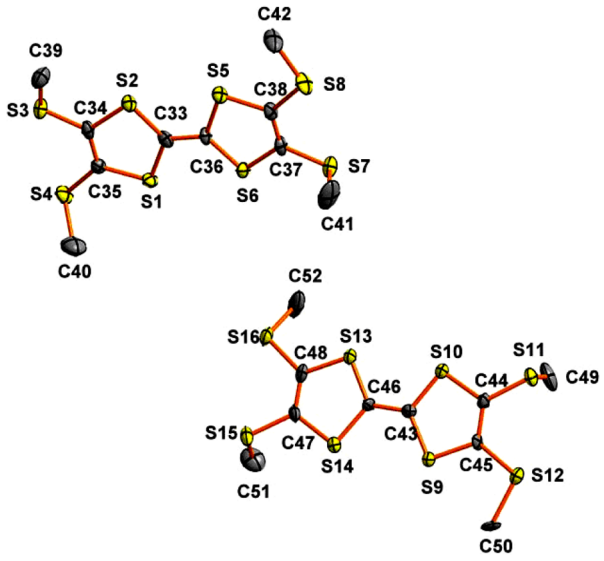

Figure 2. ORTEP diagram of $\mathbf{1}^{\bullet+}$ drawn at the 50% probability level. H atoms and anions $[Al(OR_F)_4]^-$ are omitted for clarity (S, yellow; C, gray).

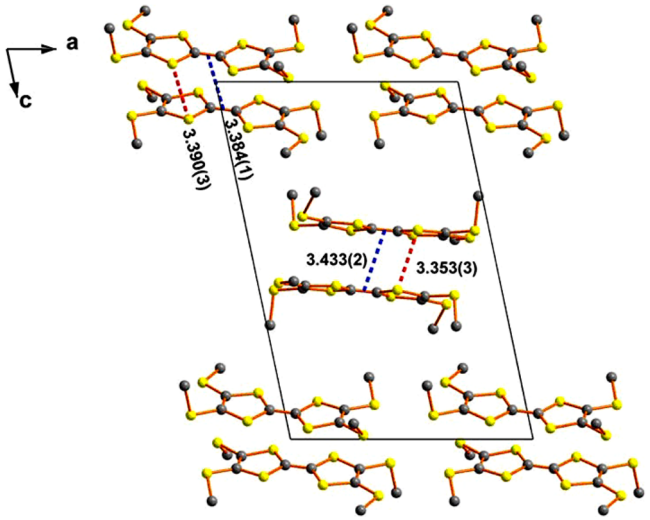

Figure 3. The extended structure of $\mathbf{1}^{\bullet+}$. H atoms and anions $[Al(OR_F)_4]^-$ are omitted for clarity. Blue lines represent the distance for π-stacking of the central C═C bond, and red lines represent the distance for shortest S···S contact (S, yellow; C, gray).

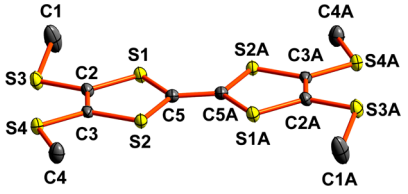

Figure 4. ORTEP diagram of $\mathbf{1}^{2+}$ drawn at the 50% probability level. H atoms and anions $[Al(OR_F)_4]^-$ are omitted for clarity (S, yellow; C, gray).

All of the compounds are thermally stable as crystals under nitrogen or argon atmosphere and can be stored for several weeks at room temperature. Since they are well-soluble in some organic solvents, more characterization in solution, for example, UV−vis−NIR, EPR, and ^{1}H NMR studies, were performed to investigate their physical and chemical properties. The X-ray single crystal structures of all compounds are also discussed.

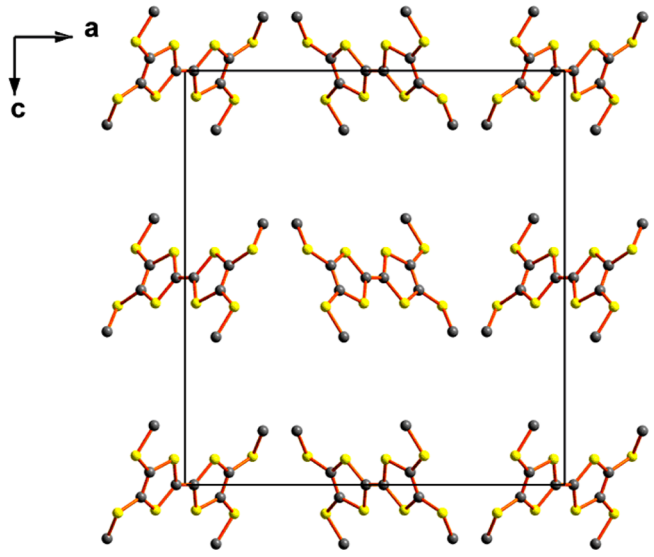

Figure 5. The extended structure of $\mathbf{1}^{2+}$. H atoms and anions $[Al(OR_F)_4]^-$ are omitted for clarity (S, yellow; C, gray).

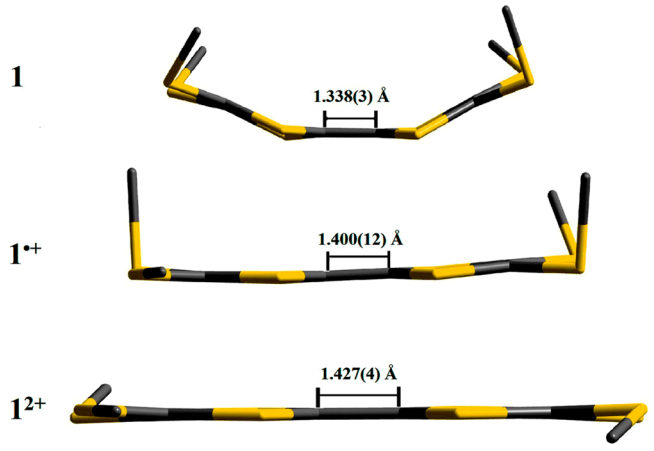

Figure 6. Molecular planar diagram for **1**, $\mathbf{1}^{\bullet+}$, and $\mathbf{1}^{2+}$.

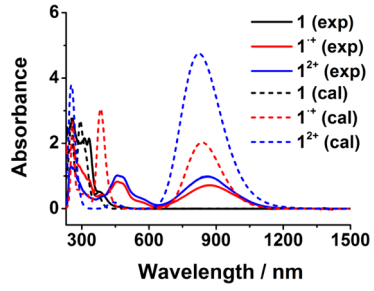

Figure 7. Experimental and calculated UV−vis−NIR absorption spectra for all of the compounds in CH_2Cl_2 at room temperature.

Crystal Structural Description. Crystals suitable for X-ray crystallographic studies were obtained by cooling solutions of corresponding compounds in CH_2Cl_2. The compounds crystallize in the monoclinic (**1**), triclinic ($\mathbf{1}^{\bullet+}$), and orthorhombic ($\mathbf{1}^{2+}$) with space group $P2_1/n$, $P\bar{1}$, and *Pbca*, respectively. Their important structural parameters are given in Table 4. In order to accurately analyze all the crystal structures

dx.doi.org/10.1021/ic5006117 | *Inorg. Chem.* 2014, 53, 5321−5327

Table 5. Selected Calculated Optical Transitions for $1^{\bullet+}$ and 1^{2+}

	orbital excitation	contribs (%)	λ/nm (calcd)	oscillator strength	λ/nm (exp)
$1^{\bullet+}$	HOMO (β) → LUMO (β)	98	837	0.2332	873
	HOMO−4 (β) → LUMO (β)	43	381	0.2971	458, 484
	HOMO (α) → LUMO+2 (α)	42			
	HOMO (α) → LUMO+1 (α)	6			
1^{2+}	HOMO → LUMO	105	823	0.6553	857
	HOMO−3 → LUMO	99	441	0.0274	458, 489

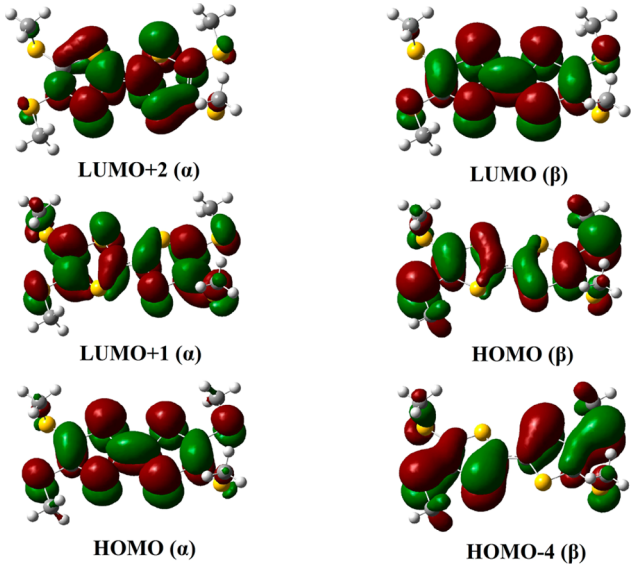

Figure 8. Selected molecular orbitals for $1^{\bullet+}$.

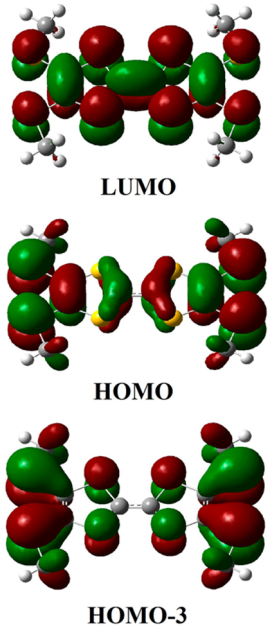

Figure 9. Selected molecular orbitals for 1^{2+}.

under the same conditions, the crystal structure of neutral TMT-TTF (**1**) was determined again at 123 K, although Zhang et al. has reported it at room temperature.[16] As shown in Figure 1, the structure of neutral TMT-TTF shows a boatlike conformation with the dihedral angle between C3−S3−S4−C4 and C7−S1−S2−C8 planes of 49.63(7)°. The central C═C bond length of the TTF core is 1.338(3) Å, and the S−C_{CH_3}

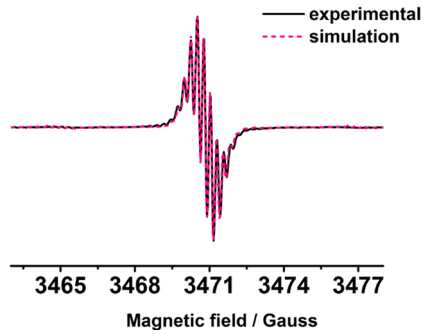

Figure 10. The EPR spectrum of $1^{\bullet+}$ in CH_2Cl_2 at room temperature (4×10^{-5} M). The black line represents experimental spectrum and the pink line represents simulation.

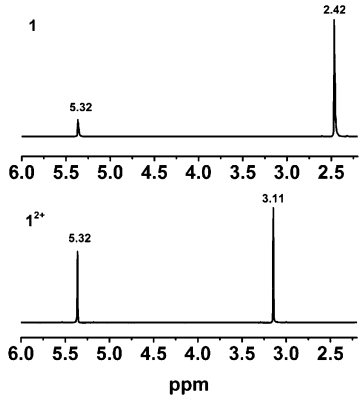

Figure 11. ^{1}H NMR of **1** and 1^{2+} in CD_2Cl_2. Peaks around 5.32 ppm are ascribed to CD_2Cl_2.

bond length ranges from 1.806(3) to 1.812(3) Å. However, no obvious intermolecular π···π and shorter S···S interactions can be observed in the packing diagram. The shortest S···S distance between two neighboring TTF cores is 4.159(1) Å (Figure S2, Supporting Information).

For $1^{\bullet+}$, there exist two TMT-TTF cations in the crystallographically independent unit with two anions $[Al(OR_F)_4]^-$ (Figure 2). The central C═C distances of the TTF units are 1.393(12) Å for C33−C36, and 1.400(12) Å for C43−C46, respectively, which are consistent with that of the similar radical compound (TMT-TTF)$[BF_4]$, as Dunbar reported.[7d] The S−C_{CH_3} bond length ranges from 1.797(11) to 1.837(11) Å. More importantly, the two five-membered rings containing S atoms are almost coplanar with the dihedral angles of 7.20(13)° for S1−C35−C34−S2 and S5−C38−C37−S6 planes and of 6.13(11)° for S13−C48−C47−S14 and S9−C45−C44−S10 planes. As illustrated in Figure 3, the extended structure constructed by the head-to-tail stacking of each two TMT-TTF cations forms the π-dimers with short S···S contact [3.390(3) and 3.353(2) Å]. It is obviously less than the sum of

dx.doi.org/10.1021/ic5006117 | Inorg. Chem. 2014, 53, 5321−5327

the van der Waals radii for two S atoms (3.70 Å). Additionally, the π stacking of the central C=C bonds can be also observed within the neighboring dimeric units with the distances of 3.384(1) and 3.433(2) Å. The results confirm the oxidized character of the TTF donor core compared with those structural parameters found in the neutral TMT-TTF and the similar TTF-derivative$^{\bullet+}$ radicals.[7c,d,17]

The reaction of neutral TMT-TTF with the stronger oxidant composition ($NOSbF_6$ and $Li[Al(OR_F)_4]$) in 1:2 ratio resulted into the formation of dication TMT-TTF^{2+}, which is rarely studied in TTF derivatives. The asymmetric unit of dication $\mathbf{1}^{2+}$ is based on half of the TMT-TTF molecule and one anion $[Al(OR_F)_4]^-$. As shown in Figure 4, the central C=C bond (C5−C5A) length for $\mathbf{1}^{2+}$ is 1.427(4) Å, obviously longer than those of **1** and $\mathbf{1}^{\bullet+}$. The distance S3−C1 is 1.797(3) Å, almost equal to the S4−C4 bond of 1.796(3) Å. Moreover, the TTF core displays perfect planarity. No intermolecular $\pi\cdots\pi$ and S···S interactions are observed for $\mathbf{1}^{2+}$ in the packing structure (Figure 5).

It is known that some structural factors, such as the central C=C bond length and the dihedral angle of the TTF core, are all charge-sensitive for the organic molecule including TTF units. As shown in Table 4 and Figure 6, there is an obvious difference for the coplanarity of the TTF core and the central C=C bond length in **1**, $\mathbf{1}^{\bullet+}$, and $\mathbf{1}^{2+}$. It should be noted that the HOMO of **1** is a combination of lone pair localized orbitals of sulfur atoms and the central C=C π-bonding orbital (Figure S3, Supporting Information). Successive removal of one electron from HOMO (hence mainly from the central C=C π-bonding orbital) of neutral TMT-TTF leads to the lengthening of the central C=C bond in the corresponding radical cation and dication.[7d]

Spectroscopic Properties. The UV−vis−NIR absorption spectra for all of the reported compounds were measured in dichloromethane solution at room temperature (Figure 7). For the neutral TMT-TTF (**1**), the electronic absorption spectrum displays intense transitions in the range 230−400 nm, which mainly come from the spin-allowed $\pi-\pi^*$ transitions.[18] Upon one-electron oxidation, strong and broad absorption bands emerge at about 873 and 458−484 nm, respectively, for $\mathbf{1}^{\bullet+}$, which are consistent with the results of previously reported similar TTF$^{\bullet+}$.[19] After further oxidation, the absorption band around 873 nm is slightly blue-shifted to 857 nm, which is attributed to the characteristic absorption for the TMT-TTF^{2+} dication ($\mathbf{1}^{2+}$). TD-DFT calculations are performed to rationalize the assignment of experimental absorption bands for $\mathbf{1}^{\bullet+}$ and $\mathbf{1}^{2+}$. The calculated absorptions and relevant molecular orbitals are shown in Table 5 and Figures 7, 8, and 9, respectively. For $\mathbf{1}^{\bullet+}$, the experimental absorption band around 458−484 nm corresponds to the predicted absorptions at 381 nm, which comes from HOMO−4 (β) → LUMO (β), HOMO (α) → LUMO+2 (α), and HOMO (α) → LUMO+1 (α), while strong absorption at 873 nm corresponds to the calculated value of 837 nm [HOMO (β) → LUMO (β)]. For $\mathbf{1}^{2+}$, the absorption peak at 857 nm can be attributed to the calculated absorptions at 823 nm with the transition from HOMO to LUMO, and the absorption around 458−489 nm mainly originates from $\pi_{TTF} \rightarrow \pi^*_{TTF}$ transitions, corresponding to the calculated peak at 441 nm with the transition HOMO−3 → LUMO.

The EPR spectrum of $\mathbf{1}^{\bullet+}$ (Figure 10) was recorded in CH_2Cl_2 at room temperature, which can be best simulated with hyperfine couplings to 12 equivalent protons [$I = {}^1/_2$, $a({}^1H)$ = 0.025 mT] from methyl groups, four equivalent sulfurs [$I = {}^3/_2$, $a({}^{33}S)$ = 0.42 mT] inside the TTF moiety, and two equivalent carbon atoms [$I = {}^1/_2$, $a({}^{13}C)$ = 0.58 mT] of the central double bond. Unresolved satellite hyperfine lines from another four sulfurs and four carbon atoms outside the TTF moiety were detected, which may be due to their positions far from the maximum of the electron spin density and their small natural abundance (^{33}S, 0.76%; ^{13}C, 1.1%).

For $\mathbf{1}^{2+}$, no EPR spectra signal can be observed at both room temperature and low temperature (77 K). But the room-temperature ^1H NMR spectrum shows a clear single peak at 3.11 ppm (Figure 11). It is slightly left-shifted compared with that of neutral TMT-TTF (δ = 2.42 ppm), which confirms the character of dication TMT-TTF^{2+}.

CONCLUSIONS

Successively chemical oxidization of the neutral tetrakis-(methylthio)tetrathiafulvalene (TMT-TTF) with suitable oxidants, including a weakly coordinating anion $[Al(OR_F)_4]^-$, results in the formation of a radical cation TMT-TTF$^{\bullet+}$ and a dication TMT-TTF^{2+}. Both TMT-TTF$^{\bullet+}$ and TMT-TTF^{2+} stabilized by the weakly coordinating anion are well-soluble in common organic solvents, which makes it is possible to investigate their physical and chemical properties in solution, as evidenced by UV−vis−NIR, ^1H NMR, and EPR studies. Single crystal X-ray diffraction analyses obviously show structural differences for all of the compounds, originating from their charge-sensitivity for this type of organic molecule involving TTF units. The foregoing results extend the further research on structure−property relations for stable organic radicals of TTF derivatives. More importantly, the synthetic method is useful for new interesting charge transfer multifunctional molecular materials.

ASSOCIATED CONTENT

Supporting Information

Supplementary table, figures, additional characterization, and X-ray crystallographic files in CIF format for all of compounds. This material is available free of charge via the Internet at http://pubs.acs.org.

AUTHOR INFORMATION

Corresponding Author

*E-mail: zuojl@nju.edu.cn; xpwang@nju.edu.cn. Fax: +86-25-83314502.

Notes

The authors declare no competing financial interest.

ACKNOWLEDGMENTS

This work was supported by the Major State Basic Research Development Program (2011CB808704 and 2013CB922101), the National Natural Science Foundation of China (51173075 and 91122019), and the Natural Science Foundation of Jiangsu Province (BK20130054). We also thank Dr. Yue Zhao and Dr. Zai-Chao Zhang for their assistance in the crystallographic work.

REFERENCES

(1) (a) Mori, T. *Chem. Rev.* **2004**, *104*, 4947−4970. (b) Coronado, E.; Day, P. *Chem. Rev.* **2004**, *104*, 5419−5448. (c) Givaja, G.; Amo-Ochoa, P.; Gómez-García, C. J.; Zamora, F. *Chem. Soc. Rev.* **2012**, *41*, 115; *Chem. Soc. Rev.* **2012**, *41*, 115−147. (d) Bogani, L.; Wernsdorfer,

W. *Nat. Mater.* **2008**, *7*, 179−186. (e) Leuenberger, M. N.; Loss, D. *Nature* **2001**, *410*, 789−793. (f) Troiani, F.; Affronte, M. *Chem. Soc. Rev.* **2011**, *40*, 3119−3129. (g) Cornia, A.; Mannini, M.; Sainctavit, P.; Sessoli, R. *Chem. Soc. Rev.* **2011**, *40*, 3076−3091.

(2) (a) Wudl, F. *Acc. Chem. Res.* **1984**, *17*, 227−232. (b) Shibaeva, R. P.; Tagubskii, E. B. *Chem. Rev.* **2004**, *104*, 5347−5378. (c) Yamada, J.; Akutsu, H. *Chem. Rev.* **2004**, *104*, 5057−5084. (d) Coronado, E.; Curreli, S.; Giménez-Saiz, C.; Gómez-García, C. J. *Inorg. Chem.* **2012**, *51*, 1111−1126. (e) Rosokha, S. V.; Kochi, J. K. *J. Am. Chem. Soc.* **2007**, *129*, 828−838. (f) Tan, L.-X.; Guo, Y.-L.; Yang, Y.; Zhang, G.-X.; Zhang, D.-Q; Yu, G.; Xu, W.; Liu, Y.-Q. *Chem. Sci.* **2012**, *3*, 2530−2541. (g) Zhang, B.; Wang, Z.-M.; Zhang, Y.; Takahashi, K.; Okano, Y.; Cui, H.-B.; Kobayashi, H.; Inoue, K.; Kurmoo, M.; Pratt, F. L.; Zhu, D.-B. *Inorg. Chem.* **2006**, *45*, 3275−3280. (h) Shirahata, T.; Shiratori, K.; Kumeta, S.; Kawamoto, T.; Ishikawa, T.; Koshihara, S.; Nakano, Y.; Yamochi, H.; Misaki, Y.; Mori, T. *J. Am. Chem. Soc.* **2012**, *134*, 13330−13340.

(3) (a) Dressel, M.; Drichko, N. *Chem. Rev.* **2004**, *104*, 5689−5716. (b) Pop, F.; Amacher, A.; Avarvari, N.; Ding, J.; Daku, L. M. L.; Hauser, A.; Koch, M.; Hauser, J.; Liu, S.-X.; Decurtins, S. *Chem.−Eur. J.* **2013**, *19*, 2504−2514. (c) Roy, S.; Mondal, S. P.; Ray, S. K.; Biradha, K. *Angew. Chem., Int. Ed.* **2012**, *51*, 12012−12015. (d) Wenger, S.; Bouit, P.; Chen, Q.; Teuscher, J.; Censo, D. D.; Humphry-Baker, R.; Moser, J.; Delgado, J. L.; Martín, N.; Zakeeruddin, S. M.; Grätzel, M. *J. Am. Chem. Soc.* **2010**, *132*, 5164−5169. (e) Martín, N.; Sánchez, L.; Herranz, M. Á.; Illescas, B.; Guldi, D. M. *Acc. Chem. Res.* **2007**, *40*, 1015−1024.

(4) (a) Lorcy, D.; Bellec, N.; Fourmigué, M.; Avarvari, N. *Coord. Chem. Rev.* **2009**, *253*, 1398−1438. (b) Iyoda, M.; Hasegawa, M.; Miyake, Y. *Chem. Rev.* **2004**, *104*, 5085−5114. (c) Enoki, T.; Miyazaki, A. *Chem. Rev.* **2004**, *104*, 5449−5478. (d) Uzelmeier, C. E.; Smucker, B. W.; Reinheimer, E. W.; Shatruk, M.; O'Neal, A. W.; Fourmigué, M.; Dunbar, K. R. *Dalton Trans.* **2006**, 5259−5268. (e) Woess, E.; Monkowius, U.; Knoer, G. *Chem.−Eur. J.* **2013**, *19*, 1489−1495. (f) Zhong, J.-C.; Misaki, Y.; Munakata, M.; Kuroda-Sowa, T.; Maekawa, M.; Suenaga, Y.; Konaka, H. *Inorg. Chem.* **2001**, *40*, 7096−7098. (g) Pointillart, F.; Le Guennic, B.; Golhen, S.; Cador, O.; Ouahab, L. *Chem. Commun.* **2013**, *49*, 11632−11634. (h) Yokota, S.; Tsujimoto, K.; Hayashi, S.; Pointillart, F.; Ouahab, L.; Fujiwara, H. *Inorg. Chem.* **2013**, *52*, 6543−6550. (i) Pointillart, F.; Le Guennic, B.; Maury, O.; Golhen, S.; Cador, O.; Ouahab, L. *Inorg. Chem.* **2013**, *52*, 1398−1408. (j) Chen, Y.; Li, C.-H.; Wang, C.-F.; Zuo, J.-L.; You, X.-Z. *Sci. China Ser. B-Chem.* **2009**, *52*, 1596−1601.

(5) (a) Martin, D.; Soleilhavoup, M.; Bertrand, G. *Chem. Sci.* **2011**, *2*, 389−399. (b) Power, P. P. *Chem. Rev.* **2003**, *103*, 789−810. (c) Geoffroy, M. *Recent Res. Dev. Phys. Chem.* **1998**, *2*, 311−321. (d) Shuvaev, K. V.; Passmore, J. *Coord. Chem. Rev.* **2013**, *257*, 1067−1091.

(6) (a) Coronado, E.; Curreli, S.; Giménez-Saiz, C.; Gómez-García, C. J.; Alberola, A.; Canadell, E. *Inorg. Chem.* **2009**, *48*, 11314−11324. (b) Guasch, J.; Grisanti, L.; Souto, M.; Lloveras, V.; Vidal-Gancedo, J.; Ratera, I.; Painelli, A.; Rovira, C.; Veciana, J. *J. Am. Chem. Soc.* **2013**, *135*, 6958−6967. (c) Calbo, J.; Aragó, J.; Otón, F.; Lloveras, V.; Mas-Torrent, M.; Vidal-Gancedo, J.; Veciana, J.; Rovira, C.; Ortí, E. *Chem.−Eur. J.* **2013**, *19*, 16656−16664. (d) Rodríguez-García, B.; Goberna-Ferrón, S.; Koo, Y.-S.; Benet-Buchholz, J.; Galán-Mascarós, J. R. *Inorg. Chem.* **2013**, *52*, 14376−14381.

(7) (a) Ferraris, J.; Cowan, D.; Walatka, W.; Perlstein, J. *J. Am. Chem. Soc.* **1973**, *95*, 948−949. (b) Lu, W.; Zhu, Q.-Y.; Dai, J.; Zhang, Y.; Bian, G.-Q.; Liu, Y.; Zhang, D.-Q. *Cryst. Growth Des.* **2007**, *7*, 652−657. (c) Pop, F.; Auban-Senzier, P.; Frackowiak, A.; Ptaszyński, K.; Olejniczak, I.; Wallis, J. D.; Canadell, E.; Avarvari, N. *J. Am. Chem. Soc.* **2013**, *135*, 17176−17186. (d) Reinheimer, E. W.; Zhao, H.-H.; Dunbar, K. R. *Synth. Met.* **2008**, *158*, 447−452.

(8) (a) Kini, A. M.; Parakka, J. P.; Geiser, U. G.; Wang, H.-H.; Rivas, F.; DiNino, E.; Thomas, S.; Dudek, J. D.; Williams, J. M. *J. Mater. Chem.* **1999**, *9*, 883−892. (b) Wang, Y.; Cui, S.-X.; Li, B.; Zhang, J.-P.; Zhang, Y. *Cryst. Growth Des.* **2009**, *9*, 3855−3858. (c) Hudhomme, P.; Le Moustarder, S.; Durand, C.; Gallego-Planas, N.; Mercier, N.; Blanchard, P.; Levillain, E.; Allain, M.; Gorgues, A.; Riou, A. *Chem.−Eur. J.* **2001**, *7*, 5070−5083.

(9) (a) Zheng, X.; Wang, X.-Y.; Qiu, Y.-F.; Li, Y.-T.; Zhou, C.-K.; Sui, Y.-X.; Li, Y.-Z.; Ma, J.; Wang, X.-P. *J. Am. Chem. Soc.* **2013**, *135*, 14912−14915. (b) Pan, X.-B.; Chen, X.-Y.; Li, T.; Li, Y.-Z.; Wang, X.-P. *J. Am. Chem. Soc.* **2013**, *135*, 3414−3417. (c) Pan, X.-B.; Su, Y.-T.; Chen, X.-Y.; Zhao, Y.; Li, Y.-Z.; Zuo, J.-L.; Wang, X.-P. *J. Am. Chem. Soc.* **2013**, *135*, 5561−5564. (d) Chen, X.-Y.; Wang, X.-Y.; Zhou, Z.-Y.; Li, Y.-Z.; Sui, Y.-X.; Ma, J.; Wang, X.-P.; Power, P. P. *Angew. Chem., Int. Ed.* **2013**, *52*, 589−592. (e) Chen, X.-Y.; Wang, X.-Y.; Sui, Y.-X.; Li, Y.-Z.; Ma, J.; Zuo, J.-L.; Wang, X.-P. *Angew. Chem., Int. Ed.* **2012**, *51*, 11878−11881. (f) Chen, X.-Y.; Ma, B.-B.; Wang, X.-Y.; Yao, S.-X.; Ni, L.-C.; Zhou, Z.-Y.; Li, Y.-Z.; Huang, W.; Ma, J.; Zuo, J.-L.; Wang, X.-P. *Chem.−Eur. J.* **2012**, *18*, 11828−11836.

(10) Gemmell, C.; Janairo, G. C.; Kilburn, J. D.; Ueck, H.; Underhill, A. E. *J. Chem. Soc., Perkin Trans. 1* **1994**, 2715−2720.

(11) Krossing, I. *Chem.−Eur. J.* **2001**, *7*, 490−502.

(12) *SAINTPLUS: Software Reference Manual*, Version 6.45; Bruker-AXS: Madison, WI, 1997−2003.

(13) Sheldrick, G. M. *SADABS*; University of Göttingen: Göttingen, Germany, 1996.

(14) Sheldrick, G. M. *SHELXS-97 and SHELXL-97, Programs for Crystal Structure Analysis*; University of Göttingen: Göttingen, Germany, 1997.

(15) Frisch, M. J.; Trucks, G. W.; Schlegel, H. B.; Scuseria, G. E.; Robb, M. A.; Cheeseman, J. R.; Scalmani, G.; Barone, V.; Mennucci, B.; Petersson, G. A.; Nakatsuji, H.; Caricato, M.; Li, X.; Hratchian, H. P.; Izmaylov, A. F.; Bloino, J.; Zheng, G.; Sonnenberg, J. L.; Hada, M.; Ehara, M.; Toyota, K.; Fukuda, R.; Hasegawa, J.; Ishida, M.; Nakajima, T.; Honda, Y.; Kitao, O.; Nakai, H.; Vreven, T.; Montgomery, J. A., Jr.; Peralta, P. E.; Ogliaro, F.; Bearpark, M.; Heyd, J. J.; Brothers, E.; Kudin, K. N.; Staroverov, V. N.; Kobayashi, R.; Normand, J.; Raghavachari, K.; Rendell, A.; Burant, J. C.; Iyengar, S. S.; Tomasi, J.; Cossi, M.; Rega, N.; Millam, N. J.; Klene, M.; Knox, J. E.; Cross, J. B.; Bakken, V.; Adamo, C.; Jaramillo, J.; Gomperts, R.; Stratmann, R. E.; Yazyev, O.; Austin, A. J.; Cammi, R.; Pomelli, C.; Ochterski, J. W.; Martin, R. L.; Morokuma, K.; Zakrzewski, V. G.; Voth, G. A.; Salvador, P.; Dannenberg, J. J.; Dapprich, S.; Daniels, A. D.; Farkas, Ö.; Ortiz, J. V.; Cioslowski, J.; Fox, D. J. *Gaussian 09*, revision A.08 ; Gaussian, Inc.: Wallingford, CT, 2009.

(16) Wang, L.; Zhang, J.-P.; Zhang, B. *Acta Crystallogr.* **2005**, *E61*, o65−o66.

(17) Boudiba, L.; Gousamia, A.; Gollen, S.; Ouahab, L. *Synth. Met.* **2011**, *161*, 1800−1804.

(18) (a) Khandar, A. A.; Shaabani, B.; Belaj, F.; Bakhtiari, A. *Inorg. Chim. Acta* **2007**, *360*, 3255−3264. (b) Wu, J.-C.; Liu, S.-X.; Keene, T. D.; Neels, A.; Mereacre, V.; Powell, A. K.; Decurtins, S. *Inorg. Chem.* **2008**, *47*, 3452−3459.

(19) Khodorkovsky, V.; Shapiro, L.; Krief, P.; Shames, A.; Mabon, G.; Gorgues, A.; Giffard, M. *Chem. Commun.* **2001**, 2736−2737.